A&A 527, A45 (2011)
DOI: 10.1051/0004-6361/201015824

Astronomy & Astrophysics

How does C^+ recombine in diffuse molecular gas?

H. S. Liszt

National Radio Astronomy Observatory, 520 Edgemont Road, Charlottesville, VA, 22903-2475, USA
e-mail: hliszt@nrao.edu

Received 27 September 2010 / Accepted 9 December 2010

ABSTRACT

Aims. We wish to understand the processes whereby the dominant state of free carbon shifts from C^+ to C I and CO in progressively denser and/or darker diffuse and translucent clouds.
Methods. We discuss recent compilations and observations of C I, H I, H_2 and CO measured in uv absorption and compare the observations with models of the thermal and ionization equilibrium including and excluding grain-assisted neutralization of atomic ions such as C^+.
Results. There are significant disparities in N(C I) and divergent behaviour with respect to H I and especially H_2 and CO in two recent discussions of the C I abundance in diffuse and translucent gas. If the older data tabulated by Wolfire et al. (2008, ApJ, 680, 384) are considered, the run of N(C I) with N(H I) and $N(H_2)$ is comfortably explained only by models embodying grain-assisted atomic-ion neutralization, much as those authors noted. If the newer data of Burgh et al. (2010, ApJ, 708, 334) are considered, either lower density models with grain-assisted atomic-ion neutralization or much denser models without it may suffice. In either case N(CO) increases from 10^{14} cm^{-2} to 10^{16} cm^{-2} with little change in N(C I) in either dataset, presenting a real challenge to models of C^+ recombination and CO formation in the $C^+ \rightarrow$ C I $\rightarrow$ CO transition.
Conclusions. N(CO) exceeds N(C I) even at $N(\mathrm{CO}) \gtrsim 3 \times 10^{15}$ cm^{-2}, well within the regime of diffuse gas where the dominant form of free gas phase carbon is C^+; one of the supposed signatures of the translucent regime, that C I is the dominant form of free carbon, is not found on the sky. However, the C I data clearly need to be put on a firmer basis before the $C^+ \rightarrow$ C I $\rightarrow$ CO transition may be understood. Ambiguities in the C I column densities determined in *uv* absorption may perhaps be resolved by sub-mm observations with *Herschel* or ALMA.

Key words. atomic processes – molecular processes – ISM: abundances – Galaxy: disk

1. Introduction

Singly-ionized carbon is responsible for the bulk of the cooling in the cool neutral phase of the interstellar medium (ISM) and it provides most of the free electrons there. Carbon monoxide, the recombination product of HCO^+ with these electrons in diffuse gas, is the dominant form of free carbon and provides the bulk of the cooling in dark gas. The $C^+ \rightarrow$ CO transition (Glassgold & Langer 1976) is now generally understood as a tiered process in which the dominant form of carbon gradually shifts from C^+ to C I to CO with increasing in situ density and extinction, i.e. as the gas changes from diffuse ($A_V \lesssim 1$ mag) to translucent to dark ($A_V \gtrsim 5$ mag) (Neufeld et al. 2005; Snow & McCall 2006). In this picture neutral atomic carbon is the dominant form of free gas-phase carbon in the translucent regime when 1 mag $\lesssim A_V \lesssim$ 3 mag.

There are many reasons to study this process but capturing the transition in observations has proved problematical on many accounts, not the least of which is the difficulty of observing all of the relevant gas constituents in the same object. Studies of mm-wave emission in translucent clouds typically find objects in which the bulk of the hydrogen is in H_2 and the free carbon is already overwhelmingly in CO, and in any case there is no straightforward way of determining the column densities of H I, H_2, C^+ or C I (and, perhaps, also CO) in such clouds; for instance see Turner et al. (2000) and references therein.

By contrast, optical/uv absorption measurements provide column densities for all the relevant gas constituents along the same sightlines but have had difficulty finding objects that obviously (in their measured properties) lie beyond the diffuse regime, even when the total line of sight extinction and H_2 column density are comparatively large (McCall et al. 2002; Rachford et al. 2009). Larger total extinction (a translucent or dark sightline) generally results from the accumulation of smaller individual contributions (which speaks to the distribution of cloud column densities).

In any case, the number of optical/uv sightlines with measured neutral carbon column densities has recently doubled (Wolfire et al. 2008; Burgh et al. 2010) and here we discuss available observations of the $C^+ \rightarrow$ C I $\rightarrow$ CO transition from several related perspectives: the physics of C^+ recombination (Wolfire et al. 2008; Bryans et al. 2009); the relationship between N(C I) and N(CO) (Burgh et al. 2010); and the formation of CO from the recombination of HCO^+ (Visser et al. 2009).

The plan of this work is as follows. Section 2 describes the sources of the data that are discussed here. Section 3 compares observations of C I with those of H I, H_2 and CO. With this background in mind, Sect. 4 discusses the underlying physics of C^+ recombination and CO formation and Sect. 5 compares the observations with models of these two processes. Section 6 is a summary and discussion.

2. Optical/uv absorption measurements

2.1. Atomic carbon and supporting information on H I and H_2

The measurements of C I lines discussed here are all available in the recent literature. In particular, Wolfire et al. (2008) recently

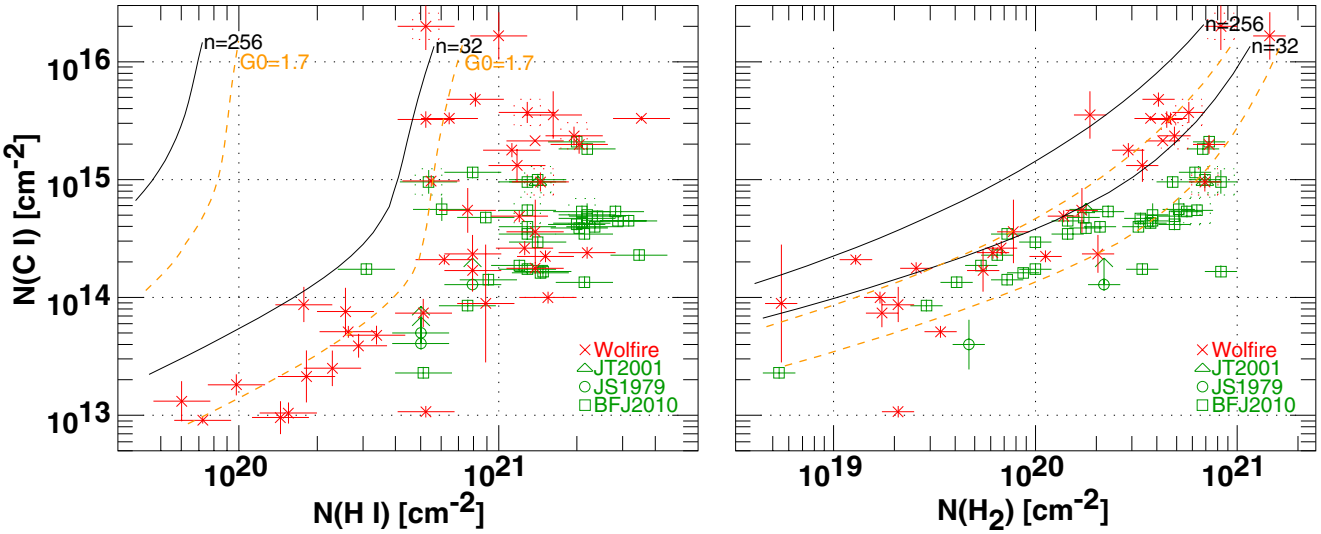

Fig. 1. Neutral atomic carbon column density related to H I and H_2. *Left*: N(C I) vs. N(H I); *Right*: N(C I) vs. $N(H_2)$. Superposed are results for models that include grain-assisted atomic-ion neutralization, at two densities $n(H) = 32$ cm^{-3} and 256 cm^{-3}, at two values of the scaling factor for the interstellar radiation field, $G_0 = 1.0$ (solid curves) and 1.7 (dashed (orange) curves). Sources of C I measurements are labelled as; WTHK08: Wolfire et al. (2008); JT2001: Jenkins & Tripp (2001); JS1979: Jenkins & Shaya (1979); BFJ2010: Burgh et al. (2010). Sightlines having two values of N(C I) (see Table 1) are enclosed by dotted rectangles at both values.

summarized the older literature, largely the data of Jenkins & Shaya (1979), and provided a comprehensive table of supporting information (A_V, N(H I), $N(H_2)$). Column densities $N(C^+)$ are measured along some lines of sight (Sofia et al. 2004; Jenkins 2009) but are not discussed here. Wolfire et al. (2008) cast their discussion in terms of the ratio N(C I)/N(C II) assuming $N(C) = 1.6 \times 10^{-4}\ N(H)$ where $N(H) = N(H\ I) + 2N(H_2)$ is the total column density of hydrogen.

Since the work of Wolfire et al. (2008), the sample of sightlines with measured N(C I) was about doubled with the work of Burgh et al. (2010) who also helpfully provided tables with supporting information including new and previously-measured values of N(CO). To complete the dataset for the present discussion we also culled from the literature a few other sightlines for which relevant supporting information could be assembled; from the work of Jenkins & Shaya (1979) the sightlines toward HD 30614, HD 57060 and HD 57061 and from the seminal study of Jenkins & Tripp (2001) the sightlines toward HD 209339 and HD 210839.

As explained by Burgh et al. (2010), their C I column densities were extracted using the methods and oscillator strengths of Jenkins & Tripp (2001), and they are systematically smaller for higher column densities than those that would have been derived using other oscillator strengths (Morton 2003) and methods. This is apparent in the discussion here but to make the point explicit, we show in Table 1 the C I column densities for those stars in common between their work and that of Jenkins & Shaya (1979) or Wolfire et al. (2008).

2.2. Carbon monoxide

Burgh et al. (2010) include a summary of measurements of N(CO), seven of which are new in their work. For the remainder of the sightlines considered here, CO column densities were taken from the recent work of Sonnentrucker et al. (2007), Burgh et al. (2007) and Sheffer et al. (2008), which had previously been summarized in Liszt (2007). We also include a small sample of sightlines observed in mm-wave CO emission and absorption, placing them in $N(H_2)$ using observations of N(CO) and $N(HCO^+)$ (Liszt & Lucas 1998) with $X(HCO^+) = N(HCO^+)/N(H_2) = 3 \times 10^{-9}$ (Liszt et al. 2010) as in the models for CO formation discussed in Sect. 4 here.

Table 1. Log N(C I)[1] from Burgh et al. (2010) and Wolfire et al. (2008).

Source	Burgh et al. (2010) dex cm^{-2}	Wolfire et al. (2008) dex cm^{-2}
HD 24534	14.98(0.10)	16.30(0.20)
HD 185418	14.74(0.05)	15.57(0.09)
HD 192639	14.73(0.05)	15.37(0.05)
HD 210839	15.00(0.05)	14.98(0.08)

Notes. [(1)] Quantities in parentheses are logarithmic uncertainties.

3. Observations of the $C^+ \rightarrow$ C I $\rightarrow$ CO transition

3.1. Carbon and hydrogen

The C I data are shown in Fig. 1 (and with different model results superposed, but otherwise identically, in Fig. 2), where N(C I) is plotted against N(H I) at left and against $N(H_2)$ at right. The graphs at right ignore sightlines having somewhat smaller N(H I) and very much smaller $N(H_2)$ but the full dataset is shown in Fig. A.1 in the Appendix.

There is a component of N(C I) that increases with N(H I) in Fig. 1 at left while $N(H\ I) \lesssim 4 \times 10^{20}$ cm^{-2} and the molecular fraction $f_{H_2} = 2N(H_2)/N(H)$ is small, but for larger N(H I) and N(C I) the scatter increases and there is no sensible relationship between N(C I) and N(H I). By contrast, at the right there are relatively tight relationships between N(C I) and $N(H_2)$, albeit very differently in the sample of Burgh et al. (2010) and otherwise. This underscores the point made long ago (Liszt 1981) that once the molecular fraction increases substantially at $N(H) > 4 \times 10^{20}$ cm^{-2} (Savage et al. 1977), the observed neutral atomic carbon occurs in regions that are strongly molecular in hydrogen, even when the overall molecular fraction along the line of sight taken as a whole is small.

Unhappily, comprehension of the general relationships between neutral atomic carbon and other species is greatly compromised by the evident disparities in the quoted C I column densities. Older data in the recent tabulation of Wolfire et al. (2008) extend to much higher values as previewed by the comments in Burgh et al. (2010). The disparity is not merely a matter of sampling, as noted in Table 1 comparing values of N(C I) for the few sightlines in common. As will be seen in Sect. 4, the disparate measurements actually call for very different physical explanations.

3.2. Carbon and carbon monoxide

Many of the sightlines with optically-measured CO column densities now also have complementary C I measurements making possible a fuller examination of the remainder of the $C^+ \rightarrow C\,I \rightarrow CO$ transition (Burgh et al. 2010). This is partly shown in Fig. 3. Note the two or more order of magnitude spread in N(CO) at $N(H_2) \gtrsim 4\times10^{20}$ cm^{-2} that in principle (see Sect. 4) could be explained either by relatively small varations in the radiation field or by order of magnitude variations in the density.

As the CO-H_2 dataset grows more comprehensive it increasingly appears that the abrupt increase in N(CO) represents a change in the underlying character of the gas, much as the abrupt increase of N(C I) at $N(H\,I) > 4\times10^{20}$ cm^{-2} in Fig. 1 signals the onset of the $H\,I \rightarrow H_2$ transition. Sheffer et al. (2008) have argued that there are two separate chemical regimes represented in Fig. 3.

In any case, there is relatively little scatter in the N(C I) – $N(H_2)$ relationships in Figs. 1–2 at $N(H_2) \gtrsim 4\times10^{20}$ cm^{-2} when the disparities in measurement techniques are taken into account. The increase of N(C I) with $N(H_2)$ is no faster than linear for the Wolfire et al. (2008) compilation and somewhat slower for the newer data of Burgh et al. (2010).

Figure 4 partly repeats the format of Fig. 1, showing N(C I) plotted against N(CO). As shown in Fig. 1 of Burgh et al. (2010) the data show astonishingly rapid increases of N(CO) with N(C I), N(CO) increasing by about a factor of 200 or more while N(C I) stagnates at 5×10^{14} cm^{-2} < N(C I) < 2×10^{15} cm^{-2} in the newer data or at slightly higher values in the compilation of Wolfire et al. (2008). Explaining this behaviour represents a serious challenge to modelling the $C^+ \rightarrow C\,I \rightarrow CO$ transition, as noted in Sect. 5.

4. C^+ recombination and CO formation

4.1. C^+

Understanding the physical processes by which carbon and other trace metal ions recombine in diffuse gas has evolved in stages from the initial consideration of purely gas-phase radiative processes in basic references like Spitzer (1978). This subject was recently discussed at length by Wolfire et al. (2008) and Bryans et al. (2009) who make the following points.

4.1.1. Recombination of carbon ions with electrons

For ions with low-lying fine-structure states (including C^+ and N^+) the process of recombination with a free electron in the gas occurs by so-called dielectronic recombination (DR) at rates (Badnell et al. 2003) that are faster than in the pure radiative case (RR) ignoring the fine-structure (Badnell 2006). For C^+ Wolfire et al. (2008) provide an analytic approximation $\alpha(T_K) = 1.8\times10^{-11}(T_K/100\,K)^{-0.83}$ cm^3 s^{-1}, which at T_K = 56 K is about 2.4 times larger than the recombination coefficient used by Morton (1975) in his classic analyis of the line of sight toward ζ Oph. The importance of dielectronic recombination for carbon ions was probably understood first in study of the low-frequency radio recombination lines of C^+ (Payne et al. 1994) and there is no doubt whatsoever that DR is operating in the diffuse ISM.

4.1.2. Carbon ions and PAH aka small grains

Moreover (again, see Wolfire et al. 2008, but also Wolfire et al. 1995; and Wolfire et al. 2003), in models of the ISM that recognize the presence of PAH or small grains for heating the gas (Bakes & Tielens 1994), gas-phase atomic ions are neutralized in interaction with PAH at rates far faster than those of either RR or DR. This process of grain-assisted atomic ion neutralization was introduced by Lepp & Dalgarno (1988b) and Lepp & Dalgarno (1988a), in part to explain the higher electron densities derived by analyis of ionization ratios like MgII/MgI or FeII/FeI compared to other diagnostics; higher neutralization rates due to grain-assisted atomic-ion neutralization imply lower and more compatible densities. This situation is encountered here in that models neglecting grain-assisted atomic-ion neutralization are not capable of explaining the neutral carbon column densities tabulated by Wolfire et al. (2008) at densities that are typical of diffuse and translucent gas as discussed in Sect. 5.2.

The rate of grain-assisted atomic-ion neutralization is proportional to the thermal velocity of the atomic ion (i.e. inversely proportional to the square-root of the atomic weight) and for lighter ions (including carbon) grain-assisted atomic-ion neutralization operates ten or more times faster than recombination with free electrons. Figure 1 of Liszt (2003) shows the relative rates of gas and grain neutralization of hydrogen as a function of density and elemental depletion and Wolfire et al. (2003) give helpful expressions that can be used to estimate the local rate of grain-assisted atomic-ion neutralization.

Neutralization occurs mostly in interactions with negatively-charged particles and the ionization balance in the grain population must be calculated self-consistently using the grain-charging formalization of Draine & Sutin (1987). Negatively-charged PAH typically dominate the small grain population but do not constitute an important repository of charge for the (diffuse) gas as a whole because the fractional abundance of small grains relative to hydrogen is $\lesssim10^{-6}$. Such anion abundances could be much more important in denser and more opaque gas where the overall ionization is dominated by cosmic rays.

The relevance of grain-assisted atomic-ion neutralization to current observations has been stressed by Liszt (2003) and Welty et al. (2003) and references there. It hardly seems possible to build workable models of the cool ISM without invoking the photoelectric effect on small grains as the main heating mechanism, in which case grain-assisted atomic-ion neutralization should also occur.

There is one other distinction between models with and without grain-assisted atomic-ion neutralization. When grain-assisted atomic-ion neutralization is included, the abundance of free protons is suppressed, so that the observed amounts of H_3^+ (McCall et al. 2002) or HD, OH^+ and OH (Liszt 2003; Gerin et al. 2010) cannot be reproduced unless the cosmic-ray ionization rate is increased. The models shown here have $\zeta_H = 10^{-17}$ s^{-1} when grain-assisted atomic-ion neutralization is neglected and $\zeta_H = 10^{-16}$ s^{-1} when it is included, where ζ_H is the cosmic-ray ionization rate per H-atom.

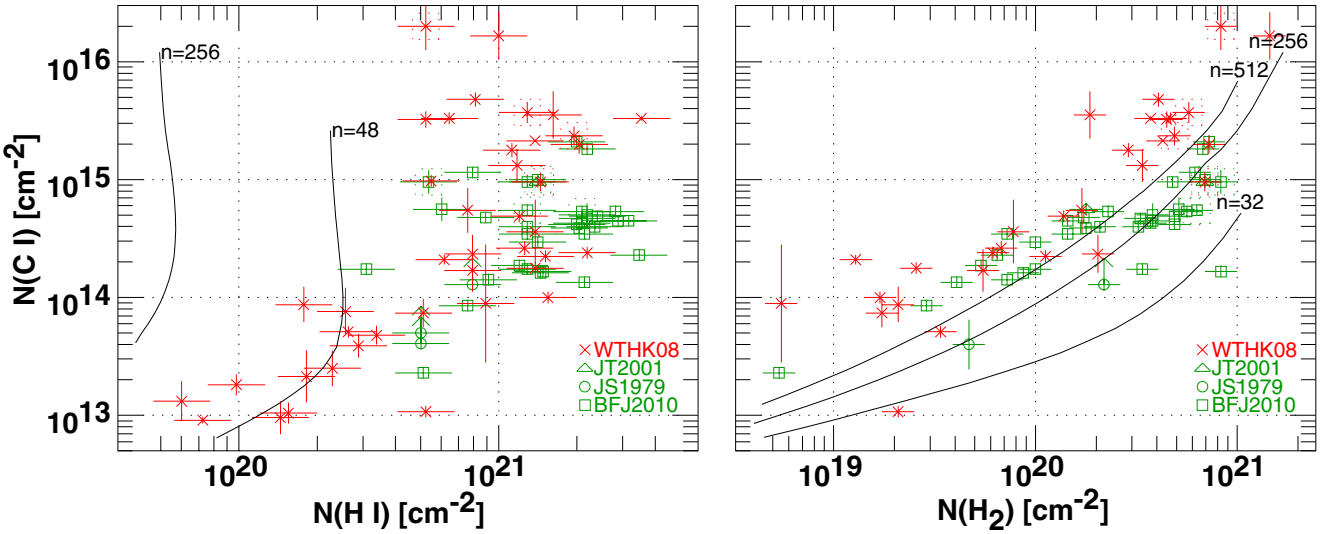

Fig. 2. Neutral atomic carbon column density related to H I and H_2. *Left*: N(C I) vs. N(H I); *Right*: N(C I) vs. $N(H_2)$. Superposed are results for models in which grain-assisted atomic-ion neutralization does not operate, at densities n(H) as indicated and for $G_0 = 1$. Sources of C I measurements are labelled as in Fig. 1.

4.2. Modelling the recombination of carbon

As noted above, Wolfire et al. (2008) discussed the neutral carbon fraction using heating/cooling models of diffuse gas embodying grain-assisted atomic-ion neutralization (Wolfire et al. 1995, 2003) but newly including H_2 formation on grains and H_2 self-shielding; they fit an overall scaling parameter $\Phi_{PAH} = 0.4$ in denser gas and $\Phi_{PAH} \approx 0.2-0.4$ otherwise, which we here take as $\Phi_{PAH} = 0.33$ always following the work of Wolfire et al. (2003). The total PAH number density and surface area are proportional to Φ_{PAH}.

We had previously duplicated the basic heating cooling calculation including H_2 and CO formation in a spherical geometry employing the H_2 and CO shielding factors of Lee et al. (1996), for instance see Liszt (2007), and further discuss such results here concerning the neutral carbon calculation. Minor differences in geometry aside, our calculations replicate the results of Wolfire et al. (2008) and fully confirm the analysis of the data that were available to them.

4.3. Modelling the formation of carbon monoxide

To complete the discussion of the $C^+ \rightarrow$ C I $\rightarrow$ CO transition it is necessary to consider observations and modelling of CO. The observational data has greatly expanded recently and the CO-H_2 comparison can now be made along almost 100 lines of sight, as shown in Fig. 3 using the previously-published data cited in Sect. 2.

As noted by Burgh et al. (2010) in their own Fig. 1, recent a priori models of CO formation chemistry may underproduce CO by a wide margin. However a simple prescription exists for forming sufficient quantities of CO, namely to allow HCO^+ to recombine quiescently with ambient electrons at the observed relative abundance $X(HCO^+) \approx 3 \times 10^{-9}$ (Liszt et al. 2010). This is shown in Fig. 3 where model results are presented for n(H) = 256 cm^{-3}, $G_0 = 1.0$ and 1.7, as will be discussed in detail in Sect. 5. The origin of the HCO^+ is something of a mystery but the CO formation problem, per se, is not.

In Sect. 5.3 below we discuss the fact that the abundance of C I fails to keep pace with that of CO when N(CO) increases rapidly at $N(H_2) \gtrsim 4 \times 10^{20}$ cm^{-2}. In this context it is important to note that the photodissociation of CO should not be an important source of neutral atomic carbon in diffuse gas. The in situ photodissociation rate must be modelled self-consistently given the CO self-shielding, but can be estimated parametrically in terms of the local formation rate (i.e. recombination of HCO^+ with an ambient electron fraction that is comparable to or slightly greater than that of C^+ or carbon as a whole) and an assumed abundance of CO. For typical fractional abundances n(CO)/n(H) $\approx 3 \times 10^{-6}$ (Burgh et al. 2010), only about 1% of the observed C I would arise from CO. Destroying CO to form C I is just not a winning proposition under these conditions.

5. Comparison of models and observations

Shown superposed in the panels of our figures are the results of models with and without grain-assisted atomic-ion neutralization (respectively using $\Phi_{PAH} = 0.33$ and $\Phi_{PAH} = 0$ see Sect. 4.2). Models have n(H) = 256 cm^{-3} and $G_0 = 1.0$ unless otherwise indicated. With grain-assisted atomic-ion neutralization some models are also shown for larger $G_0 = 1.7$ and for smaller n(H) = 32 cm^{-3} because these are the adjustments that better fit disparate portions of the data. Without grain-assisted atomic-ion neutralization, models are shown for lower and higher density n(H) = 32 and 512 cm^{-3}, but not for the stronger radiation field. Comparing Figs. 1 and 2 in the region of smaller N(H I), one sees for example that at N(H I) = 10^{20} cm^{-2} the models using grain-assisted atomic-ion neutralization have about five times higher N(C I) at slightly smaller density.

5.1. Atomic carbon and hydrogen

The lower density models with grain-assisted atomic-ion neutralization and n(H) = 32 cm^{-3} mimic the basic form of the C I-H I relationship in Fig. 1 in the left panel, i.e. a proportionality where f_{H_2} is small (N(H) $\lesssim 4 \times 10^{20}$ cm^{-2}) and an abrupt rise at slightly larger N(H I) where $N(H_2)$ increases abruptly. At smaller N(H I) the data can be fit with grain-assisted atomic-ion neutralization at $G_0 = 1$ and n(H) $\lesssim 12$ cm^{-3} or (as shown) at slightly higher density with correspondingly higher G_0. Models lacking grain-assisted atomic-ion neutralization reproduce the

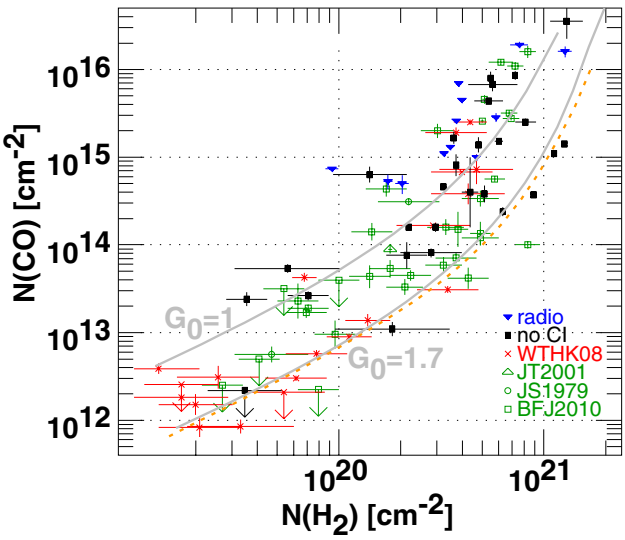

Fig. 3. Column density of carbon monoxide vs. that of H_2. Data for CO were taken from Sonnentrucker et al. (2007), Burgh et al. (2007), Sheffer et al. (2007), Sheffer et al. (2008) and Burgh et al. (2010) and sources with measured N(C I) are labelled as in Fig. 1. Sources labelled "radio" are taken from Liszt & Lucas (1998) assuming $X(HCO^+) = 3 \times 10^{-9}$; sources with measured N(C I) are called out as in Fig. 1. Steady-state, self-consistent model results (solid curves) are shown for $n(H) = 256$ cm^{-3}, $G_0 = 1$ and 1.7 under the assumption that HCO^+ recombines with electrons in thermal equilibrium at the local kinetic temperature for this value of $X(HCO^+)$, see Sect. 3 of the text. The dashed (orange) curve is for $G_0 = 1$ and $n(H) = 32$ cm^{-3}, illustrating the extreme sensitivity of X(CO) to the radiation field.

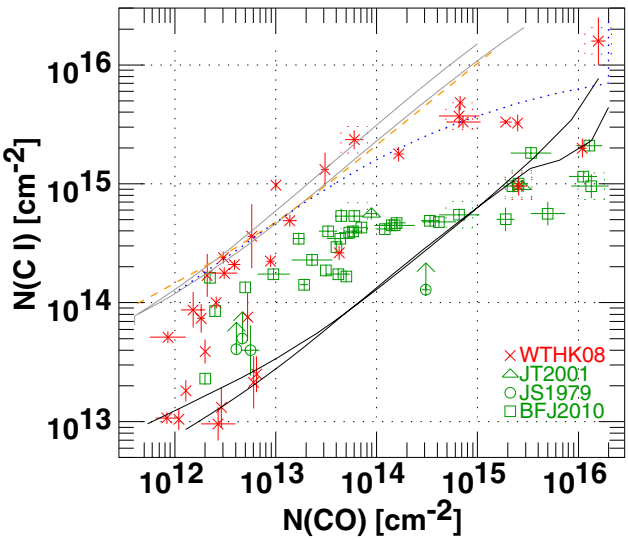

Fig. 4. Neutral atomic carbon related to carbon monoxide. Also shown are model results with and without grain-assisted atomic-ion neutralization. Models with active grain-assisted atomic-ion neutralizationshown in solid gray and dashed orange curves have the parameters used in Fig. 3. The blue dotted curve with grain-assisted atomic-ion neutralization allows the ambient *uv* radiation to ionize carbon almost without attenuation. Models with inactive grain-assisted atomic-ion neutralizationare shown for $n(H) = 32$ cm^{-3} and 512 cm^{-3} at $G_0 = 1$. Sources of C I data are labelled as in Fig. 1.

C I observations at $N(H\ I) < 3 \times 10^{20}$ cm^{-2} data with $n(H) \approx 50$ cm^{-3} and we could not find a way to push them to explain the abrupt increase in N(C I) at slightly larger N(H I).

5.2. Neutral carbon and molecular hydrogen

Perhaps the most telling result in Fig. 1 is the curve for $n(H) = 256$ cm^{-3} and $G_0 = 1.7$ at right, which passes through the majority of the data discussed by Wolfire et al. (2008) using basically the same parameters they employed to fit an improved value of Φ_{PAH}. The model results using grain-assisted atomic-ion neutralization are physically plausible and need few adjustments to explain the entirety of the data they considered. However, it is also possible to fit the newer data, using lower densities; the same model with grain-assisted atomic-ion neutralization at $n(H) = 32$ cm^{-2} and $G_0 = 1.7$ that explains the run of N(C I) vs. N(H I) at left in Fig. 1 would need only minor adjustments to explain the behaviour of N(C I) with $N(H_2)$ as well. The densities in those models would be rather small and the temperatures consequently high, given that the thermal pressures are in the range derived by Jenkins & Tripp (2001) from studies of C I fine-structure excitation.

By contrast, attempts to fit the N(C I)–$N(H_2)$ relationships in the absence of grain-assisted atomic-ion neutralization produce somewhat implausible results. With regard to the tabulation of Wolfire et al. (2008), very high densities $n(H) \gg 512$ cm^{-3} and/or weak radiation fields $G_0 < 1$ are needed; this is the fundamental problem recognized by Lepp & Dalgarno (1988b) and Lepp & Dalgarno (1988a). On the other hand, attempts to explain the newer data of Burgh et al. (2010) are implausible in that they require progressively higher density for the data at smaller $N(H_2)$ and N(C I) (where lower densities might have been expected).

5.3. Neutral carbon and CO

Shown in Fig. 4 are comparisons of the neutral carbon and CO column densities with model results with and without grain-assisted atomic-ion neutralization. As shown by the near coincidence of the curves for varying physical parameters in the two cases, we found it essentially impossible to change the model results in the N(C I)–N(CO) plane by varying the gas density or incident radiation field. The models which produce such different results in Fig. 3 (showing N(CO) vs. $N(H_2)$) produce overlapping results in Fig. 4. This insensitivity presumably ocurs because CO and C I are both formed by recombination with the same pool of electrons and both are destroyed by uv photons.

The model results with and without grain-assisted atomic-ion neutralization have the same slope but pass through very different portions of one or other of the datasets. The model results can be displaced vertically by varying the strength of the grain-assisted atomic-ion neutralization and the assumed abundance of HCO^+ but in no case do they produce such rapid increases of N(CO) at constant N(C I) as seem to be present in either dataset. Recall that the models being fit have constant number density and varying column density and extinction, so N(C I) will increase somewhat faster than linearly with N(H), but this is hardly apparent in Fig. 4. The sharp increase in N(CO) at $N(H_2) \gtrsim 4 \times 10^{20}$ cm^{-2} and the failure of N(C I) to keep up (as the models would demand) are separate mysteries.

The failure of N(C I) to increase with N(CO) is not due to C I destruction in any obvious chemical reaction. We tinkered with the models to ascertain the required rate and shown in Fig. 4 are results for the contrived case where the attenuation of the carbon-ionizing radiation alone was reduced to nearly zero; instead of varying as $2.2 \times 10^{-10}\ \exp(-2.6A_V)$ s^{-1}, we

used 2.2×10^{-10} exp$(-0.26A_V)$ s^{-1}, roughly equivalent to an added destruction rate per atom of 2×10^{-10} s^{-1}. With a typical ion-molecule reaction rate constant 2×10^{-9} cm^3 s^{-1} and $n(H_2) = 100$ cm^{-3} the fractional abundance of any prospective reaction partner relative to H_2 would have to be of order 0.001, an impossibly high value. On the "supply-side" of this issue, there is no evidence that C^+ ever disappears from the gas phase over the range of A_V considered here (Jenkins 2009), as would be required in order to shut off the supply of C I.

The abrupt increase of N(CO) at $N(H_2) \gtrsim 4 \times 10^{20}$ cm^{-2} is not uniquely observed in *uv* absorption. CO, CS, HCN, C_2H, NH_3, H_2CO and other species observed at mm-wavelengths in absorption toward quasars all increase abruptly in column density by about a factor of ten at $N(HCO^+) = 1{-}2 \times 10^{12}$ cm^{-2} or $N(H_2) \approx 3{-}6{\times}10^{20}$ cm^{-2}, for instance see Liszt et al. (2006) and references there. Conversely, CH and OH show no perturbation in their near-linear variation with $N(H_2)$ over the same interval (Liszt 2007; Weselak et al. 2009, 2010).

6. Summary

There are fundamental disparities in the C I column density data represented by the tabulation of Wolfire et al. (2008) and the new results of Burgh et al. (2010) and also in the physics required to interpret them, as illustrated in Figs. 1 and 2 and discussed here in Sects. 3–5. Given the disagreements for the few targets where the datasets overlap (see Table 1) and the very different observed behaviour when C I is compared with H I and H_2, it seems that at least one of the sets of observational results is simply wrong. Until this matter is settled, progress in understanding the $C^+ \rightarrow$ C I $\rightarrow$ CO transition will likely be stalled.

If the matter is decided in favor of results like those compiled by Wolfire et al. (2008), the physics of C^+ recombination make a strong case for the operation of grain-assisted atomic-ion neutralization as Wolfire et al. (2008) discussed and as we also showed here in Sect. 4. If the methods and oscillator strengths of Jenkins & Tripp (2001) prevail, as employed by by Burgh et al. (2010), the C I, H I and H_2 data may be interpreted using models with or without grain-assisted atomic-ion neutralization, but at very low density in the first case and at very high density (especially for diffuse clouds) in the latter.

The comparison of C I and CO column densities presents another problem, albeit somewhat more strikingly for the data of Burgh et al. (2010). At $N(H_2) \gtrsim 4{-}6 \times 10^{20}$ cm^{-2} N(CO) increases by two or more orders of magnitude with little increase at all in N(C I), which is not easily reproduced in models that otherwise might seem to account for the general variation of either C I or CO with H_2 individually (see Figs. 1–2 and Sect. 4, or Figs. 3 and 4 and Sect. 5 respectively).

No matter which C I dataset is considered, $N(CO) \gtrsim N$(C I) when $N(CO) \gtrsim 3 \times 10^{15}$ cm^{-2}, well within the diffuse regime where the dominant form of gas phase carbon is C^+: 98% at $A_V = 1$ if $N(CO) = N(C\ I) = 3 \times 10^{15}$ cm^{-2}. In the usual view of the $C^+ \rightarrow$ C I $\rightarrow$ CO transition $N(CO) < N$(C I) until well after the extinction is so high that the dominant form of gasesous carbon is C I, i.e. at $N(C\ I) \gtrsim 10^{18}$ cm^{-2} (see Fig. 1 of Snow & McCall 2006). One of the usual presumed hallmarks of the translucent cloud regime, where the dominant from of free carbon is C I rather than C^+ or CO, really does not exist on the sky in available data.

Of course one must hope that the manifest ambiguities of the existing C I data will be resolved. However, it is also possible that ambiguities in the C I column density will be resolved by observation of the 492 and 809 GHz C I fine-structure lines by sensitive modern instruments such as *Herschel* and ALMA, along lines of sight where at least the column density of CO may be ascertained.

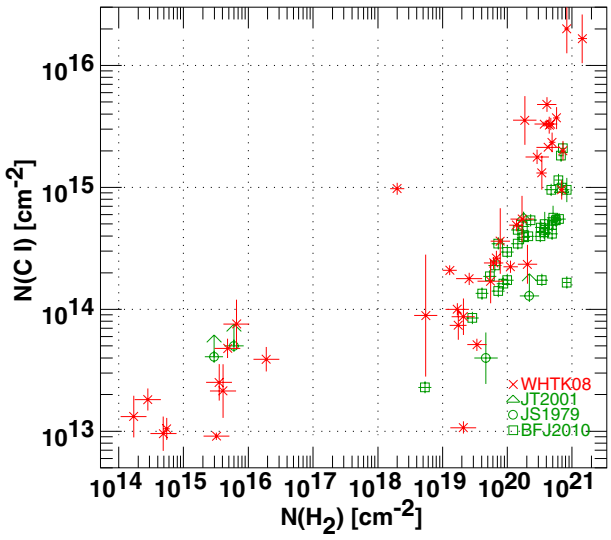

Fig. A.1. C I and H_2 column densities over the full range of $N(H_2)$ not shown in Figs. 1 and 2 of the text. Sources of C I data are labelled as in Fig. 1.

Acknowledgements. The National Radio Astronomy Observatory is operated by Associated Universites, Inc. under a cooperative agreement with the US National Science Foundation. Sympathetic and perceptive comments from the editor and an anonymous referee were gratefully received.

Appendix A: The full variation of N(C I) with $N(H_2)$

Shown in Fig. A.1 are C I and H_2 column densities over the full range of $N(H_2)$ not shown in Fig. 1 of the text. In this view, N(C I) appears to increase very rapidly with $N(H_2)$ for $N(H_2) > 10^{19}$ cm^{-2} but comparison with CO (Fig. 4 of the text) shows that N(CO) varies much more rapidly still.

References

Badnell, N. R. 2006, Ap&SS, 167, 334
Badnell, N. R., O'Mullane, M. G., Summers, H. P., et al. 2003, A&A, 406, 1151
Bakes, E. L. O., & Tielens, A. G. G. M. 1994, ApJ, 427, 822
Bryans, P., Kreckel, H., Roueff, E., Wakelam, V., & Savin, D. W. 2009, ApJ, 694, 286
Burgh, E. B., France, K., & McCandliss, S. R. 2007, ApJ, 658, 446
Burgh, E. B., France, K., & Jenkins, E. B. 2010, ApJ, 708, 334
Draine, B. T., & Sutin, B. 1987, ApJ, 320, 803
Gerin, M., de Luca, M., & Black, J. 2010, A&A, 518, L110
Glassgold, A. E., & Langer, W. D. 1976, ApJ, 206, 85
Jenkins, E. B. 2009, ApJ, 700, 1299
Jenkins, E. B., & Shaya, E. J. 1979, ApJ, 231, 55
Jenkins, E. B., & Tripp, T. M. 2001, Ap&SS, 137, 297
Lee, H. H., Herbst, E., Pineau Des Forets, G., Roueff, E., & Le Bourlot, J. 1996, A&A, 311, 690
Lepp, S., & Dalgarno, A. 1988a, ApJ, 335, 769
Lepp, S., & Dalgarno, A. 1988b, ApJ, 324, 553
Liszt, H. 2003, A&A, 398, 621
Liszt, H., Lucas, R., & Pety, J. 2006, A&A, 448, 253
Liszt, H., Pety, J., & Lucas, R. 2010, A&A, 518, A45
Liszt, H. S. 1981, ApJ, 246, L147
Liszt, H. S. 2007, A&A, 476, 291
Liszt, H. S., & Lucas, R. 1998, A&A, 339, 561
McCall, B. J., Hinkle, K. H., Geballe, T. R., et al. 2002, ApJ, 567, 391
Morton, D. C. 1975, ApJ, 197, 85
Morton, D. C. 2003, Ap&SS, 149, 205
Neufeld, D. A., Wolfire, M. G., & Schilke, P. 2005, ApJ, 628, 260

Payne, H. E., Anantharamaiah, K. R., & Erickson, W. C. 1994, ApJ, 430, 690
Rachford, B. L., Snow, T. P., Destree, J. D., et al. 2009, Ap&SS, 180, 125
Savage, B. D., Drake, J. F., Budich, W., & Bohlin, R. C. 1977, ApJ, 216, 291
Sheffer, Y., Rogers, M., Federman, S. R., Lambert, D. L., & Gredel, R. 2007, ApJ, 667, 1002
Sheffer, Y., Rogers, M., Federman, S. R., et al. 2008, ApJ, 687, 1075
Snow, T. P., & McCall, B. J. 2006, ARA&A, 44, 367
Sofia, U. J., Lauroesch, J. T., Meyer, D. M., & Cartledge, S. I. B. 2004, ApJ, 605, 272
Sonnentrucker, P., Welty, D. E., Thorburn, J. A., & York, D. G. 2007, Ap&SS, 168, 58
Spitzer, L. 1978, Physical processes in the interstellar medium (New York: Wiley-Interscience), 333
Turner, B. E., Herbst, E., & Terzieva, R. 2000, Ap&SS, 126, 427
Visser, R., van Dishoeck, E. F., & Black, J. H. 2009, A&A, 503, 323
Welty, D. E., Hobbs, L. M., & Morton, D. C. 2003, Ap&SS, 147, 61
Weselak, T., Galazutdinov, G., Beletsky, Y., & Krełowski, J. 2009, A&A, 499, 783
Weselak, T., Galazutdinov, G. A., Beletsky, Y., & Krełowski, J. 2010, MNRAS, 402, 1991
Wolfire, M. G., Hollenbach, D., McKee, C. F., Tielens, A. G. G. M., & Bakes, E. L. O. 1995, ApJ, 443, 152
Wolfire, M. G., McKee, C. F., Hollenbach, D., & Tielens, A. G. G. M. 2003, ApJ, 587, 278
Wolfire, M. G., Tielens, A. G. G. M., Hollenbach, D., & Kaufman, M. J. 2008, ApJ, 680, 384